Bioorg. Med. Chem. 72 (2022) 116964

Contents lists available at ScienceDirect

Bioorganic & Medicinal Chemistry

journal homepage: www.elsevier.com/locate/bmc

1,2,4-Triazole-3-thione analogues with an arylakyl group at position 4 as metallo-β-lactamase inhibitors

Laurent Gavara [a,*], Federica Verdirosa [b], Laurent Sevaille [a], Alice Legru [a], Giuseppina Corsica [b], Lionel Nauton [c], Paola Sandra Mercuri [d], Filomena Sannio [b], Filomena De Luca [b], Margot Hadjadj [a], Giulia Cerboni [b], Yen Vo Hoang [a], Patricia Licznar-Fajardo [e], Moreno Galleni [d], Jean-Denis Docquier [b,f,*], Jean-François Hernandez [a,*]

[a] Institut des Biomolécules Max Mousseron, Univ Montpellier, CNRS, ENSCM, Montpellier, France
[b] Dipartimento di Biotecnologie Mediche, Università di Siena, I-53100 Siena, Italy
[c] Institut de Chimie de Clermont-Ferrand, Université Clermont-Auvergne, CNRS, Clermont-Ferrand, France
[d] Laboratoire des Macromolécules Biologiques, Centre d'Ingénierie des Protéines-InBioS, Université de Liège, Institute of Chemistry B6a, Sart-Tilman, 4000 Liège, Belgium
[e] HSM, Univ Montpellier, CNRS, IRD, CHU Montpellier, France
[f] Laboratoire de Bactériologie Moléculaire, Centre d'Ingénierie des Protéines-InBioS, Université de Liège, B-4000 Liège, Belgium

ARTICLE INFO

This work is dedicated to the memory of a friend and former colleague, Dr Otto Dideberg.

Keywords:
Metallo-β-Lactamase
1,2,4-triazole-3-thione
Bacterial resistance
β-lactam antibiotic

ABSTRACT

Metallo-β-lactamases (MBLs) represent an increasingly serious threat to public health because of their increased prevalence worldwide in relevant opportunistic Gram-negative pathogens. MBLs efficiently inactivate widely used and most valuable β-lactam antibiotics, such as oxyiminocephalosporins (ceftriaxone, ceftazidime) and the last-resort carbapenems. To date, no MBL inhibitor has been approved for therapeutic applications. We are developing inhibitors characterized by a 1,2,4-triazole-3-thione scaffold as an original zinc ligand and few promising series were already reported. Here, we present the synthesis and evaluation of a new series of compounds characterized by the presence of an arylalkyl substituent at position 4 of the triazole ring. The alkyl link was mainly an ethylene, but a few compounds without alkyl or with an alkyl group of various lengths up to a butyl chain were also synthesized. Some compounds in both sub-series were micromolar to submicromolar inhibitors of tested VIM-type MBLs. A few of them were broad-spectrum inhibitors, as they showed significant inhibitory activity on NDM-1 and, to a lesser extent, IMP-1. Among these, several inhibitors were able to significantly reduce the meropenem MIC on VIM-1- and VIM-4- producing clinical isolates by up to 16-fold. In addition, ACE inhibition was absent or moderate and one promising compound did not show toxicity toward HeLa cells at concentrations up to 250 μM. This series represents a promising basis for further exploration. Finally, molecular modelling of representative compounds in complex with VIM-2 was performed to study their binding mode.

1. Introduction

Carbapenemases, or carbapenem-hydrolysing β-lactamases, are enzymes belonging to several molecular classes (e. g. the class A KPC-type, the class B VIM- and NDM-types and the class D OXA-type enzymes such as OXA-48 or OXA-40), which are able to efficiently inactivate carbapenems. Carbapenems, a sub-class of β-lactam antibiotics, typically show highly potent and broad-spectrum antibacterial activity against

Abbreviations: ACE, angiotensin-converting enzyme; *CLSI*, Clinical and Laboratory Standards Institute; *DCM*, dichloromethane; *DFT*, density functional theory; *DMF*, dimethylformamide; *DMSO*, dimethylsulfoxide; *DPT*, di(2-pyridyl) thionocarbonate; *FIC*, fractional inhibitory concentration; *HEPES*, 4-(2-Hydroxyethyl)-1-piperazine-ethanesulfonic acid; *IMP*, imipenemase; *KPC*, *Klebsiella pneumoniae* Carbapenemase; *MBL*, metallo-β-lactamase; *MEM*, meropenem; *MIC*, minimum inhibitory concentration; *NDM*, New Delhi Metallo-β-lactamase; *OXA*, oxacillinase; *PDB*, protein data bank; *SBL*, serine-β-lactamase; *VIM*, Verona Integron-borne Metallo-β-lactamase.

* Corresponding authors at: Institut des Biomolécules Max Mousseron, Univ Montpellier, CNRS, ENSCM, Montpellier, France (L. Gavara & J.-F. Hernandez), Dipartimento di Biotecnologie Mediche, Università di Siena, I-53100 Siena, Italy (J.-D. Docquier).
E-mail addresses: laurent.gavara@umontpellier.fr (L. Gavara), jddocquier@unisi.it (J.-D. Docquier), jean-francois.hernandez@umontpellier.fr (J.-F. Hernandez).

https://doi.org/10.1016/j.bmc.2022.116964
Received 29 March 2022; Received in revised form 22 July 2022; Accepted 6 August 2022
Available online 11 August 2022

relevant opportunistic pathogens, and are thus considered last resort therapeutics for the treatment of serious infections caused by antibiotic-resistant bacteria. In addition, some carbapenemases exhibit a broad-substrate profile, thus conferring resistance to other β-lactams antibiotics, such as penicillins and the widely used oxyiminocephalosporins. [1–3] Their rapid spread among multidrug-resistant opportunistic Gram-negative pathogens rapidly evolving towards ultra- and pan-drug resistance phenotypes is of major concern and exacerbates the current scarcity of therapeutic solutions useful to treat nosocomial infections caused by such ultra-resistant isolates. This alarming perspective has now been globally acknowledged for a few years, and the World Health Organization (WHO) has designated the fight against carbapenem-resistant Gram-negative bacteria (*Acinetobacter baumannii*, *Pseudomonas aeruginosa* and *Enterobacterales*) as a critical priority for antibiotic discovery and development. [4].

Carbapenemases are divided into two large families of hydrolases depending on their catalytic mechanism. [5] Those using a catalytic serine belong to either molecular class A (e. g. KPC-type) or class D (e. g. OXA-48-type) serine-β-lactamases (SBL). [6] Metallo-β-lactamases (MBLs) are zinc-dependent hydrolases and belong to molecular class B. [7] Three distinct MBL subclasses are known (B1, B2, and B3), which show different zinc requirements, active site architecture and substrate profiles. [8] Acquired MBLs are increasingly found in Gram-negative bacteria, subclass B1 VIM-, NDM-, and IMP-types being the most clinically relevant enzymes. These are highly worrying because of their broad substrate profile, their global spreading not only in the hospital setting but also in the community, [9] and the absence of approved inhibitors. Indeed, this situation contrasts with the recent approval of several β-lactamase inhibitors (e. g. avibactam and vaborbactam) targeting SBL-type carbapenemases, most notable KPC-type enzymes and OXA-48. [10,11].

Identifying a broad-spectrum inhibitor targeting both all subclass B1 enzymes, ideally the VIM-, NDM- and IMP-type MBLs, is a challenge because of the significant structural differences within their active sites. [10,12,13] The majority of reported MBL inhibitors contain a zinc-coordinating group and many different metal-binding pharmacophores have been utilized. [14] Among the most frequently reported are the thiol group [15–18] and the carboxylate group, single or multiple. [19,20] While the majority of inhibitors forms ternary complexes with their targets, some act by zinc stripping, [21–23] with potential risk of insufficient selectivity toward human metallo-enzymes. [24].

Currently, the most advanced inhibitors[25] are the thiazole-4-carboxylate ANT2681, which preclinical evaluation was recently achieved[26] and the bicyclic boronates taniborbactam[27–30] and QPX7728. [31] In particular, the latter are ultrabroad-spectrum inhibitors of both serine- and metallo-carbapenemases and taniborbactam associated to cefepime is currently under phase III clinical trials in patients with complicated urinary tract infections.

Several other series of compounds possessing a heterocycle as a zinc ligand have also been reported. [32–36] In particular, since the discovery by an in silico study that a 1,2,4-triazole-3-thione compound could inhibit a MBL (i.e. the B3 sub-class L1), [32] this scaffold has retained much attention. A crystallographic study showed that this heterocyclic motif simultaneously coordinated the two zinc ions present in the L1 active site by its N^2 and S^3 atoms. [37] The same original binding mode was later observed within the active sites of the B1 sub-class VIM-2[38–41] and NDM-1[40] enzymes. These studies as well as other random virtual and experimental screenings, which also included IMP-1 support that the 1,2,4-triazole-3-thione scaffold is well adapted for binding the dinuclear active site of these enzymes. [40,42,43].

We already reported several series of 1,2,4-triazole-3-thione compounds diversely substituted at positions 4 and 5 and identified in each of these series potent inhibitors with a more or less large spectrum of activity against MBLs of high clinical impact (i.e. VIM-, NDM- and IMP-type). [39,41,44–46] Among these, a few compounds were found to reduce the minimum inhibitory concentration (MIC) of meropenem toward multi-resistant VIM-type MBL-producing clinical isolates up to 16-fold. However, none showed synergistic activity on NDM-1-producing clinical isolates. The main reasons were probably their insufficient capacity to penetrate and/or a too low inhibition potency for the enzyme ($K_i > 1$ μM). For instance, we reported Schiff base analogues (Fig. 1A, C, D) as potent and broad-spectrum inhibitors. [39] Unfortunately, none could potentiate the antibacterial activity of meropenem against any MBL-producing clinical isolate. To solve this strong limitation, we are developing series of compounds where the hydrazone-like bond (i.e. N = CH) was replaced by a stable CH_2-CH_2 link. We recently reported a series of inhibitors derived from a Schiff base sub-family represented by the compound shown in Fig. 1A (i.e. with a 2-(*o*-benzoic)ethyl group at position 4 as in Fig. 1B). [46] Whereas some analogues showed synergistic activity on VIM-producing clinical isolates, the inhibition spectrum was restricted to VIM-type enzymes and all compounds were only moderately or not active against NDM-1, in contrast to their Schiff base counterparts.

We now report on a series of new stable 4-phenethyl analogues of 1,2,4-triazole-3-thione-based Schiff base inhibitors belonging to sub-families represented by compounds shown in Fig. 1C (i.e. 2,4-dihydroxyphenyl at position 4) and 1D (i.e. *p*-benzyloxyphenyl at position 4). We also widened the variety of aryl substituents at position 4 and changed the length of the alkyl segment between the aryl group and the triazole (Fig. 1E). Overall, the synthetic compounds showed lower to similar inhibitory potencies against both tested enzymes compared to the Schiff base analogues. However, compared to the 4-[2-(*o*-benzoic) ethyl] series a few of them exhibited a broader spectrum of inhibition, including on both VIM-type MBLs, NDM-1 and IMP-1. In addition, some compounds showed synergistic activity against VIM-producing *K. pneumoniae* clinical isolates.

2. Results and discussion

2.1. Chemistry

The formation of the 1,2,4-triazole-3-thione ring was performed following the general pathway described in Scheme 1. [47] Amines R^2-NH_2 were first reacted with dipyridylthionocarbonate (DPT) to yield the intermediate isothiocyanates, which were subsequently treated in the same pot with hydrazides R^1-$CONHNH_2$ to form the thiosemicarbazide derivatives. Their cyclodehydration under basic conditions led to the expected 1,2,4-triazole-3-thione compounds.

The hydrazide R^1-$CONHNH_2$ precursors of substituent at position 5 were obtained in two steps from the corresponding carboxylic derivatives R^1-CO_2H via the ethyl ester followed by hydrazine treatment as previously described. [45,48] Most amine R^2-NH_2 precursors of the substituent at position 4 were commercially available. A few of them were prepared in two steps from the corresponding benzaldehydes as described in Scheme 2A. In this pathway, a benzaldehyde derivative was first treated with nitromethane and ammonium acetate in acetic acid to give the nitro-alkenes **1**–**6**, which were reduced to the amines **7**–**12** using $LiAlH_4$.

The amine precursor of compounds **25**, **33**, **37**, **39**, **44**, **46**, **48** and **51** (Table 1) was the 3-(aminomethyl)-1(3*H*)-isobenzofuranone **14**. Compound **14** was obtained from 2-carboxybenzaldehyde (Scheme 2B). Nitromethanation of this compound did not lead to the nitro-alkene product as seen in Scheme 2A but to the lactone **13** by reaction between the intermediate hydroxyl group and the carboxylic function. **13** was then reduced to give **14** as described in Scheme 2B.

In the case of compounds possessing a 2-(dihydroxyphenyl)ethyl at position 4 (2,4- for **21**, **38**, **41**, **45**, 2,3- for **42**, 3,4- for **43** (Table 1)), it was not possible to prepare the corresponding amine precursors 2-(dihydroxyphenyl)ethan-1-amine by following the general pathway. Indeed, the nitromethanation of the corresponding aldehyde was not efficient. Therefore, these amine precursors were obtained from the protected dihydroxybenzaldehydes. Two kinds of protected derivatives were used. The 2-(2,4-bis(benzyloxy)phenyl)ethan-1-amine **9** was used

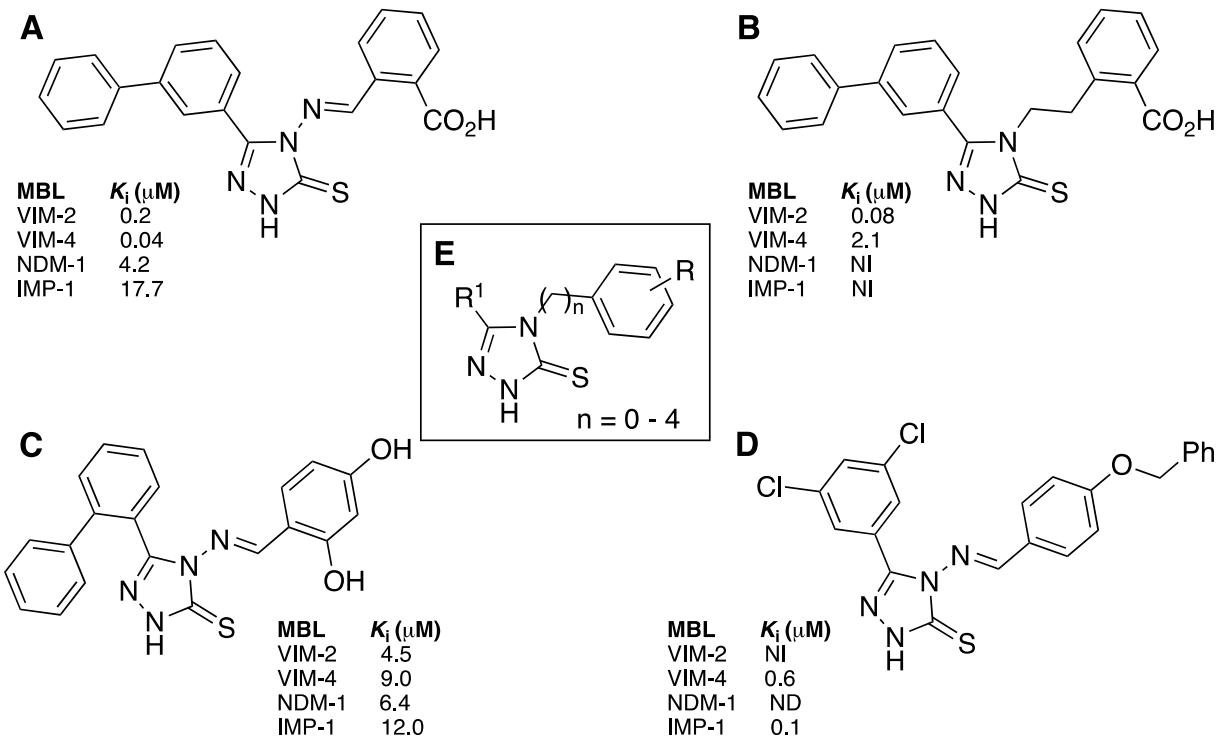

Figure 1. Structure of previously reported 1,2,4-triazole-3-thione Schiff base analogues with diverse 4-substituents[39] (A, C, D) and of a 2-(*o*-benzoic)ethyl-containing analogue [46] (B) and their inhibitory potency on selected MBLs, and general structure of synthesized analogues with an arylalkyl substituent at position 4 (E). NI, No or poor inhibition (<30 % at 100 μM). ND, Not determined.

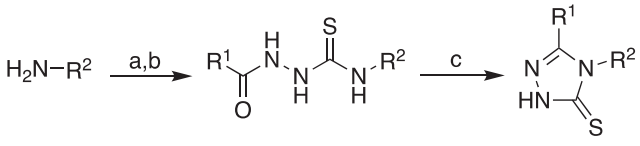

Scheme 1. Synthesis of 4-phenylalkyl-1,2,4-triazole-3-thione derivatives. *Reagents and conditions: (a) DPT, DMF, sealed tube, 55 °C, 3 h; (b) R^1-CONHNH$_2$, DMF, 55 °C, 3 h; (c) aqueous KOH or NaHCO$_3$, 100 °C, 3 h.*

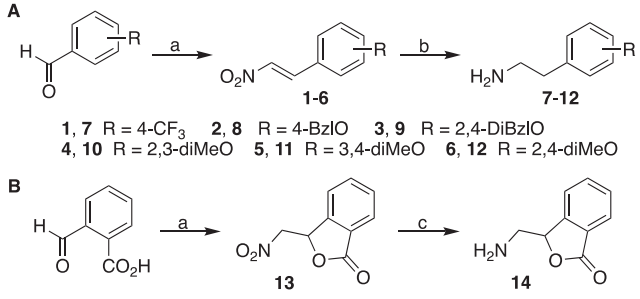

Scheme 2. Synthesis of the phenethylamines R^2-NH$_2$ **7**–**12** (A) and **14** (B). *Reagents and conditions: (a) Nitromethane, NH$_4$AcO, AcOH, 120 °C, 15 h; (b) LiAlH$_4$, THF, 80 °C, 15 h; (c) AcOH, HCl, Zn powder, 16 h, r.t.*

for the synthesis of compounds **21**, **38** and **41**, first yielding the protected intermediates. A final deprotection step was therefore carried out. However, while hydrogenolysis in the presence of a palladium catalyst was not possible because of the sulphur, other usual acidic conditions, including the use of the mixture HBr/AcOH, led to poor yields. Indeed, we observed the formation of an important secondary product resulting from the irreversible migration of one protecting benzyl group to an adjacent aromatic carbon. This unwanted reaction was reduced and yields were improved by using $AlCl_3$ in the presence of *N,N*-dimethylaniline (Scheme 3). [49] In this reaction, $AlCl_3$ is supposed to coordinate the benzyl ether oxygen atom followed by the nucleophilic addition of *N,N*-dimethylaniline on the benzyl CH_2 group, leading to the cleavage of the ether bond. Compounds **42**, **43** and **45** were prepared from the corresponding 2-(dimethoxyphenyl)ethan-1-amines **10** (2,3-dimethoxy), **11** (3,4-dimethoxy) and **12** (2,4-dimethoxy), respectively. In this case, the final methoxy cleavage was performed using boron tribromide (Scheme 4).

2.2. Evaluation of inhibitory potency toward purified MBLs.

Compounds were tested against up to five representative subclass B1 MBLs, including VIM-1, VIM-2, VIM-4, NDM-1 and IMP-1 (Tables 1 and 2). The compounds presented in Table 2 were also tested against the subclass B3 MBL L1 but were all poorly active (≤45 % inhibition at 100 μM) or inactive against this enzyme. Testing was first performed at one concentration (100 or 200 μM) and K_i values were measured for compounds exhibiting > 75 % inhibition at these concentrations.

The results obtained for a first series of 37 compounds (**15**–**51**) are presented in Table 1. The substituent at position 5 of the triazole ring was chosen among aromatic groups, which were previously found to be favourable for MBL inhibition. In addition to phenyl, it also included *o*-toluyl, 2-hydroxy-5-methoxy-phenyl, naphth-2-yl, *o*-, *m*- and *p*-biphenyl, *N*-methyl-pyrrol-2-yl, benzyl and naphth-2-ylmethyl. At position 4, compounds **15**–**51** possessed a phenethyl-derived substituent. As mentioned above, the choice of these substituents was initially based on the previously published Schiff base series[39] and included a 2,4-dihydroxyphenyl and a *p*-benzyloxyphenyl group. However, a larger panel of substituents was explored as a function of their commercial availability. In addition, because nitromethanation of 2-carboxybenzaldehyde led to an isobenzofuranone group instead of the desired nitro-alkene derivative, several compounds incorporating this substituent were prepared (i.e. **25**, **33**, **37**, **39**, **44**, **46**, **48**, **51**).

Overall, although some compounds were not active or were modest inhibitors of all tested enzymes (e.g. **17**, **24**, **39**, **47**, **49**–**51**), the others

Table 1
Inhibitory activity of 1,2,4-triazole-3-thiones **15–51** with combined R^1 and phenethyl-based R^2 against various MBLs.

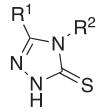

Cpd	Structure		K_i (μM)[a] or (% inhibition at [b]100 or [c]200 μM)				
	R^1	R^2	VIM-1	VIM-2	VIM-4	NDM-1	IMP-1
15		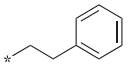	3.2 ± 0.2	NI[d]	2.1 ± 0.2	NI	NI
16		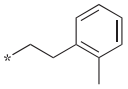	ND[e]	NI	ND	NI	NI
17		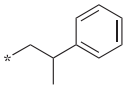	ND	NI	NI	NI	(55 %)[a]
18		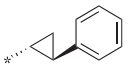	3.1 ± 0.2	(30 %)[b]	NI	15.4 ± 3.1	ND
19		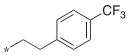	ND	NI	ND	NI	NI
20		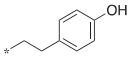	2.1 ± 0.4	6.1 ± 0.4	2.3 ± 0.1	12.0 ± 2.2	42.0 ± 3.5
21		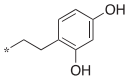	5.1 ± 0.4	NI	4.1 ± 0.3	42[f]	27.0 ± 4.2
22		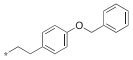	(34 %)[b]	18.9 ± 0.5	NI	NI	5.3 ± 1.8
23		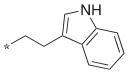	(50 %)[b]	(50 %)[c]	(50 %)[c]	NI	NI
24		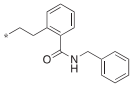	ND	NI	NI	(45 %)[b]	(45 %)[b]
25		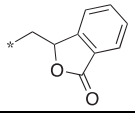	0.75 ± 0.10	NI	7.8 ± 0.7	(51 %)[b]	NI
26		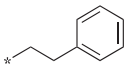	3.3 ± 0.2	9.4 ± 0.9	2.4 ± 0.2	NI	14[f]
27		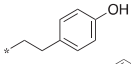	ND	ND	1.6 ± 0.1	NI	(56 %)[b]
28		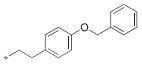	(47 %)[b]	NI	NI	NI	NI
29	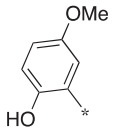	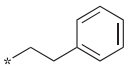	1.9 ± 0.2	3.9 ± 0.2	1.5 ± 0.1	6.8 ± 0.9	20.2 ± 1.0
30		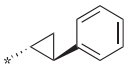	2.2 ± 0.1	(41 %)[b]	2.5 ± 0.1	9.5 ± 2.4	4.6 ± 0.3
31		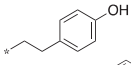	1.6 ± 0.1	3.9 ± 0.3	1.9 ± 0.1	NI	NI
32		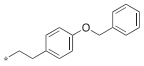	11.1 ± 0.6	NI	0.54 ± 0.03	NI	(35 %)[b]
33		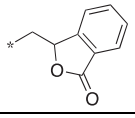	1.2 ± 0.1	3.3 ± 0.2	0.9 ± 0.1	(68 %)[b]	(47 %)[b]
34	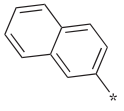	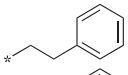	3.7 ± 0.4	NI	NI	NI	NI
35		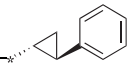	ND	NI	(35 %)[b]	NI	NI

(*continued on next page*)

Table 1 (*continued*)

Cpd	Structure		K_i (μM)[a] or (% inhibition at [b]100 or [c]200 μM)				
	R^1	R^2	VIM-1	VIM-2	VIM-4	NDM-1	IMP-1
36		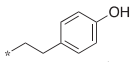	3.3 ± 0.2	NI	3.2 ± 0.2	NI	24.0 ± 2.8
37		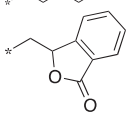	6.3 ± 2.0	NI	8.2 ± 0.8	28[f]	9.8 ± 2.1
38	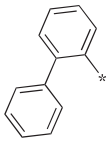	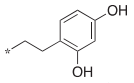	27.0 ± 1.9	(35 %)[b]	60.0 ± 2.0	15.2 ± 1.1	NI
39		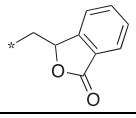	(30 %)[b]	NI	(34 %)[a]	NI	(54 %)[b]
40	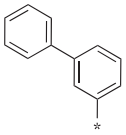	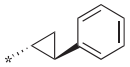	ND	NI	NI	(69 %)[b]	NI
41		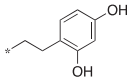	0.41 ± 0.07	1.3 ± 0.4	0.82 ± 0.07	14.3 ± 3.2	NI
42			0.70 ± 0.07	1.8 ± 0.1	0.80 ± 0.05	22.4 ± 2.5	20.0 ± 3.4
43		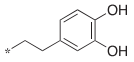	1.3 ± 0.1	1.7 ± 0.1	0.68 ± 0.05	17.4 ± 2.2	9.2 ± 0.9
44		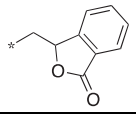	ND	NI	ND	NI	NI
45	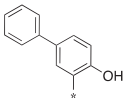	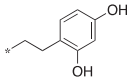	0.76 ± 0.05	1.9 ± 0.2	0.85 ± 0.05	(38 %)[b]	(44 %)[b]
46	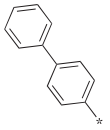	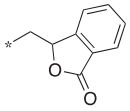	ND	NI	ND	NI	(48 %)[b]
47	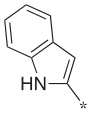	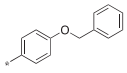	NI	NI	NI	NI	NI
48		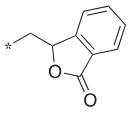	2.2 ± 0.1	(38 %)[b]	2.5 ± 0.2	(31 %)[b]	(30 %)[b]
49	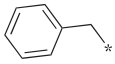	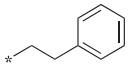	NI	NI	NI	NI	NI
50	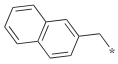	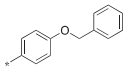	NI	NI	NI	NI	NI
51		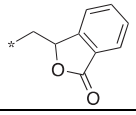	NI	NI	NI	NI	(30 %)[b]

[a] Kinetics were monitored at 30 °C by following the absorbance variation observed upon reporter substrate hydrolysis. K_i's were determined when inhibition > 75 % and values are mean ± SD. Assays performed in triplicate.
[b] Percentage of inhibition in the presence of 100 μM of inhibitor.
[c] Percentage of inhibition in the presence of 200 μM of inhibitor.
[d] No or poor inhibition (<30 % or < 50 % inhibition at 100 or 200 μM, respectively).
[e] Not determined.
[f] Apparent K_i value, not determined due to non linear v_0/v_i *vs* [I] plot.

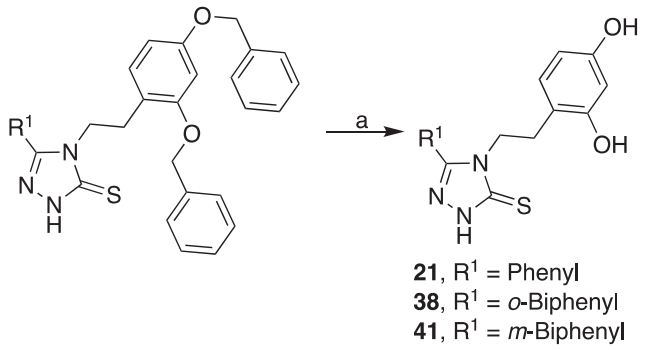

Scheme 3. Cleavage of *O*-benzyl protecting groups for the preparation of compounds **21**, **38**, **41**. *Reagents and conditions: (a) N,N-Dimethylaniline, $AlCl_3$, DCM, r.t., 10–20* min.

inhibited at least one tested enzyme with K_i values in the micromolar to submicromolar range (0.41 to 42 μM). Among these, several strongly inhibited one to both tested VIM-type enzymes only (i.e. **15**, **25**, **27**, **31**–**33**, **45**, **48**). Furthermore and most interestingly, 15 compounds (i.e. **18**, **20**–**22**, **26**, **29**, **30**, **36**, **37**, **38**, **41**–**43**) exhibited a broader spectrum of inhibition, with a detectable inhibitory activity on either NDM-1 or IMP-1, or both, in addition to inhibiting one to both tested VIM-type enzymes. This is in contrast with the series of 4-[2-(*o*-benzoic)ethyl] compounds, which displayed a restricted inhibition spectrum (i.e. potent inhibition of VIM-type enzymes but not of NDM-1 or IMP-1), [46] suggesting that the presence of a carboxylic group was not favorable for NDM-1 and IMP-1 inhibition in the 4-phenethyl series.

Although no general rule could be drawn from the study of structure–activity relationships, potent inhibitors in this series often showed a *m*-biphenyl (**41**–**43**, **45**) or 2-hydroxy-4-methoxy-phenyl (**29**–**33**) substituent as R^1, and phenethyl (**15**, **26**, **29**) or a hydroxylated phenethyl (**20**, **21**, **31**, **36**, **41**–**43**, **45**) substituent as R^2. Some of these substituents were already shown favourable in the parent Schiff base series. [39] In addition, the constrained phenethyl analogues phenylcyclopropyl (**18**, **30**) and phthalidylmethyl (**25**, **33**, **37**, **48**) were often well accommodated. Interestingly, one of the most potent IMP-1 inhibitor (i.e. **22**, K_i value of 5.3 μM) possessed a *p*-benzyloxyphenyl at position 4, previously found the most favourable for IMP-1 inhibition in the same Schiff base series. [39].

Among the active compounds, it is noteworthy that they often exhibited a better inhibition of VIM-1 and VIM-4 enzymes than of VIM-2 (e. g. **15**, **21**, **30**, **32**, **36**, **37**, **48**). This different behaviour may come from the existence of residue variability in the VIM-type MBL active sites as for instance the presence of Val223 and His224 residues for VIM-1 and VIM-4, where Ile and Tyr are found in VIM-2, respectively. In fact, all potent VIM-2 inhibitors (K_i values in the low micromolar range) were also potent VIM-1/4 inhibitors and they often displayed a hydroxylated phenethyl moiety at position 4 (i.e. **20**, **31**, **41**–**43**, **45**).

Finally, the most interesting inhibitors were compounds **20** (phenyl in 5, *p*-hydroxyphenethyl in 4), **29** (2-hydroxy-4-methoxy-phenyl in 5, phenethyl in 4), **42** and **43** (*m*-biphenyl in 5, 2,3- or 3,4-dihydroxyphenethyl in 4, respectively.) as they displayed submicromolar to micromolar K_i values against all five enzymes. In addition, although inactive against IMP-1, compound **41** (*m*-biphenyl in 5 and 2,4-dihydroxyphenethyl in 4) potently inhibited all VIM-type enzymes and to a lesser extent NDM-1 (K_i value of 14.3 μM). Compound **30** (2-hydroxy-4-methoxy-phenyl in 5, cyclopropylphenyl in 4) also showed, despite being poorly active on VIM-2, among the lowest measured K_i values (<10 μM) on NDM-1 and IMP-1, while retaining potent inhibitory activity on VIM-1 and VIM-4. These results further highlight the potential of triazole-thione compounds to be successfully optimized and yield broad-spectrum MBL inhibitors.

A second series of 11 related analogues (**52**–**62**) was prepared to explore the importance of the alkyl link between N^4 of the triazole ring and a phenyl group, substituted or not (Table 2). This link was either absent (**52**, **53**) or being one (**54**–**59**), three (**60**, **61**), or four carbon atoms-long (**62**). None of these compounds potently inhibited NDM-1, IMP-1 (with the exception of compound **54**) or the B3 subclass MBL L1. More interesting results were obtained for VIM-type enzymes, whatever the link length. In particular, several compounds (**55**, **56**, **58**, **60**, **62**) strongly inhibited both VIM-type enzymes with K_i values in the micromolar to submicromolar range. The absence of link (i.e. **52**, **53**) was the least favourable, while a benzyl moiety allowed potent VIM inhibition (i.e. **54**–**56**, **58**).

Again, VIM-2 behaved differently than VIM-1 and VIM-4 as it was not inhibited by compound **54**. In this sub-series, VIM-2 inhibition was promoted by either a carboxylic group attached to the 4-benzyl group (i. e. **55**, **56**) or by methoxy and/or hydroxy group(s) present on the 5-phenyl substituent (i.e. **58**). In fact, a methoxy group at this position in the Schiff base analogue JMV4690 was shown to establish an important hydrogen bond with the indole NH group of Trp87 in the VIM-2 active site (pdb code 6YRP[39]). Compared to the corresponding 4-phenethyl compound **15** (i.e. phenyl ring in both 4- and 5-substituents), the further increase of the alkyl chain length with one (compound **60**) or two (compound **62**) carbon atom(s) led to high inhibitory potency against all VIM-type MBLs. Compounds **60** and **62** are among the best VIM-type MBL inhibitors in this series. It is interesting to note that one previously reported analogue only differing from **62** by the presence of a sulfur instead of one CH_2 behaved similarly with regard to VIM-type enzymes. [41] Therefore, this substituent configuration might be the basis for a future series. Finally, as already observed for compounds **49**–**51** (Table 1) a benzyl group at position 5 (i.e. **59**, **61**) was not favourable to MBL inhibition.

2.3. *In vitro antibacterial synergistic activity*

A total of 20 compounds (Table 3) were selected on the basis of their inhibitory activity to evaluate their antibacterial synergistic activity with meropenem (a carbapenem antibiotic) on MBL-producing multidrug-resistant clinical isolates (VIM-1- and VIM-4-producing *K. pneumoniae* and NDM-1-producing *E. coli*). We first checked that none of the tested compounds showed intrinsic antibacterial activity

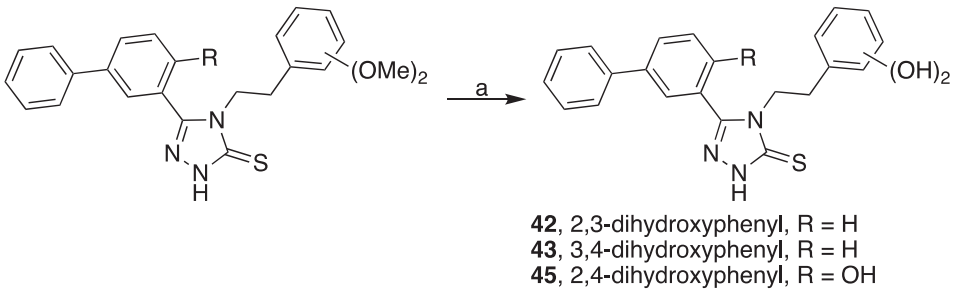

Scheme 4. Cleavage of dimethoxy groups for the preparation of compounds **42**, **43**, **45**. *Reagents and conditions: (a) 1 M BBr_3 in dry DCM, 0 °C then r.t. overnight.*

Table 2
Inhibitory activity of 1,2,4-triazole-3-thiones **42**–**62** with combined R^1 and R^2 against various MBLs.

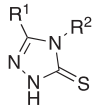

Cpd	Structure		K_i (μM)[a] or (% inhibition at 100 μM)					
	R^1	R^2	VIM-1	VIM-2	VIM-4	NDM-1	IMP-1	L1
52			3.2 ± 0.1	16.0 ± 1.0	NI[b]	NI	(30 %)	NI
53		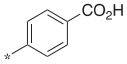	ND[c]	ND	NI	NI	NI	NI
54		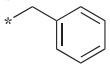	0.72 ± 0.04	NI	1.5 ± 0.1	NI	8.0 ± 0.8	(35 %)
55		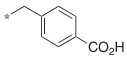	3.6 ± 0.3	2.7 ± 0.2	1.1 ± 0.1	NI	NI	(45 %)
56		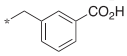	1.4 ± 0.1	1.8 ± 0.1	0.40 ± 0.02	NI	NI	ND
57		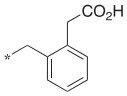	NI	(50 %)	NI	NI	NI	NI
58	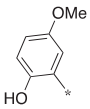	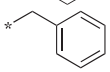	0.59 ± 0.20	4.0 ± 0.6	1.8 ± 0.8	NI	NI	(40 %)
59	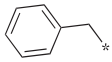		23.0 ± 3.0	NI	NI	NI	(57 %)	(40 %)
60		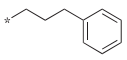	0.56 ± 0.09	0.74 ± 0.04	0.90 ± 0.10	NI	14.0 ± 1.7	NI
61	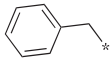		(30 %)	NI	NI	NI	(63 %)	(32 %)
62		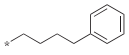	1.2 ± 0.1	0.23 ± 0.02	0.43 ± 0.03	(55 %)	NI	(50 %)

[a] Kinetics were monitored at 30 °C by following the absorbance variation observed upon reporter substrate hydrolysis. K_i's were determined when inhibition > 75 % and values are mean ± SD. Assays performed in triplicate.
[b] No or poor inhibition (<30 % at 100 μM).
[c] Not determined.

when tested alone (MIC > 128 μg/mL). MIC values of meropenem in the absence and presence of inhibitors (tested at a fixed concentration of 32 μg/mL to allow direct comparison with previously reported data [41,45,46]) were determined using the CLSI broth microdilution method and are reported in Table 3. Some compounds (e. g. **15**, **25**, **31**, **33**, **45**, **48**, **56**, **58**, **60**) were able to reduce the MIC of meropenem by 8 to 16-fold on both *K. pneumoniae* isolates (Table 3). Four to eightfold MIC reduction on both VIM-1- and VIM-4-producing bacteria was also observed for compounds **21**, **29**, **30**, **41**, **55** and **62**. Curiously, the **41** isomers **42** and **43** showed similar potentiation activity as **41** on the VIM-4-producing clinical isolate as expected (similar K_i values on VIM-4) but are inactive on the VIM-1-producing one, despite close K_i values on this enzyme. This might potentially rely on strain-specific factors, such as the composition of the outer membrane (OMPs, lipopolysaccharides) considering that these two strains were epidemiologically unrelated and may show significantly different genotypes. Furthermore, these two compounds contain a catechol moiety, which can potentially act as a siderophore group known to improve uptake through bacterial membranes via the iron acquisition system. [50] These results would not support a drastic improvement of the synergistic activity (only **43** showed a slightly better activity than **41**) when a catechol group is present in this series of triazole-thione analogues. Overall, no clear correlation between structure, inhibitory potencies and microbiological activity could be drawn. Finally, no significant activity was observed on the NDM-1-producing *E. coli* isolate, very probably because most of these compounds are less potent NDM-1 inhibitors.

In contrast with the Schiff base analogues, [39] none of which showing potentiation activity in similar assays, many compounds in this series did prove to significantly decrease the meropenem MIC. These results confirmed the beneficial effect of replacing the hydrazone-like bond by a non-hydrolysable one. Furthermore, a chequerboard analysis was carried out with meropenem and compounds **43** and **60**, selected based on their potentiation activity and availability, using the VIM-4 producing *K. pneumoniae* clinical isolate (VA-416/02). With both compounds, an average FIC index ≤ 0.5 was determined (0.48 and 0.25 for **43** and **60**, respectively), supporting a synergistic drug-drug interaction between the MBL inhibitor and the antibiotic. [51].

2.4. Inhibitor selectivity and ACE inhibition

To probe the selectivity of some representative compounds, selected based on their activity in microbiological assays and chemical diversity, an Angiotensin-Converting Enzyme (ACE, a Zn-dependent peptidase) inhibition test was carried out with a fluorogenic substrate (see

Table 3
Antibacterial synergistic activity of compounds on VIM-1- and VIM-4-producing *K. pneumoniae* and NDM-1-producing *E. coli* clinical isolates with meropenem determined by the broth microdilution method.

Cpd (32 μg/mL)	MEM MIC (μg/mL)[a] and K_i (μM) values of selected inhibitors					
	K. pneumoniae 7023 (bla^{+}_{VIM-1})		*K. pneumoniae* VA416/02 (bla^{+}_{VIM-4})		*E. coli* SI-004 M (bla^{+}_{NDM-1})	
	MEM MIC	K_i (μM)[b]	MEM	K_i (μM)	MEM	K_i (μM)
None	16	–	16	–	64	–
15	2	3.2 ± 0.2	2	2.1 ± 0.1	64	NI[c]
20	4	2.1 ± 0.4	4	2.3 ± 0.1	64	12.0 ± 2.2
21	4	5.1 ± 0.4	2	4.1 ± 0.2	ND[d]	42
25	2	0.75 ± 0.10	2	7.8 ± 0.7	64	(51 %)[e]
26	4	3.3 ± 0.2	4	2.4 ± 0.2	ND	NI
29	4	1.9 ± 0.2	2	1.5 ± 0.1	64	6.8 ± 0.9
30	4	2.2 ± 0.1	2	2.5 ± 0.1	32	9.5 ± 2.4
31	2	1.6 ± 0.1	2	1.9 ± 0.1	ND	NI
33	2	1.2 ± 0.1	2	0.93 ± 0.04	64	(68 %)[e]
41	2	0.41 ± 0.07	4	0.82 ± 0.07	32	14.3 ± 3.2
42	16	0.70 ± 0.07	4	0.80 ± 0.05	32	22.4 ± 2.5
43	16	1.3 ± 0.1	2	0.68 ± 0.05	32	17.4 ± 2.2
45	1	0.76 ± 0.05	2	0.85 ± 0.05	64	(38 %)[e]
48	2	2.2 ± 0.1	2	2.5 ± 0.2	32	(31 %)[e]
54	4	0.72 ± 0.04	4	1.5 ± 0.1	ND	NI
55	4	3.6 ± 0.3	2	1.1 ± 0.1	64	NI
56	2	1.4 ± 0.1	2	0.40 ± 0.02	32	NI
58	2	0.59 ± 0.20	2	1.8 ± 0.8	32	NI
60	2	0.56 ± 0.09	2	0.90 ± 0.10	64	NI
62	2	1.2 ± 0.1	4	0.43 ± 0.03	64	(55 %)[e]

[a] MEM, meropenem.
[b] From Tables 1 and 2.
[c] No or poor inhibition (<30 % at 100 μM).
[d] Not determined.
[e] Percentage of inhibition in the presence of 100 μM of inhibitor.

Experimental section 4.2.3 for details). Captopril, a potent inhibitor of ACE was used as the inhibition control and showed 96 % inhibition of ACE when tested at a final concentration of 100 nM. Compounds **33**, **41**, **54**, **56** and **60**, all showing among the best potentiation of meropenem in microbiological assays, were tested at 100 μM. Compounds **33**, **54** and **56** did not show any inhibitory activity on ACE, while **41** and **60** showed a moderate inhibition of the enzyme, with a percentage of inhibition equal to 35 and 50 %, respectively (SD < 10 %). Although it is difficult to provide a structural basis for these results, it could be noted that the compounds showing moderate ACE inhibition are characterized by a higher number of carbon atoms (2 or 3) separating the triazole-thione moiety from the aryl group in the R^2 side chain than that in inactive molecules (1 carbon atom). Interestingly, the extent of ACE inhibition seems to increase with the length of the alkyl linker, likely allowing a better flexibility of the R^2 substituent and thus potentially a better accommodation in the ACE active site. Nonetheless, the selectivity of the tested compounds for metallo-β-lactamases remains favorable. Indeed, and assuming a competitive mechanism of inhibition, the resulting K_i values (≈30 and 55 μM for **60** and **41**, respectively; computed using a K_m value of ACE for the fluorogenic tripeptide substrate equal to 110 μM[52]) would be at least ≈30-fold higher than the inhibition constants observed on VIM-type MBLs.

2.5. Cytotoxicity assays on human cells

The potential cytotoxicity of compound **41** was assessed using a membrane integrity assay (HeLa cells). **41** was found to not induce cell lysis at concentrations up to 250 μM. This result was confirmed using a cell viability assay (HeLa cells, 1,500 cells/well), in which no cytotoxic effects could be observed after up to 72 h of incubation in the presence of 250 μM of this compound. It is in agreement with the absence of cytotoxicity generally observed for previous series. [39,41,45].

2.6. Molecular modelling

We investigated the putative binding mode of compounds **41**, **56** and **62** within VIM-2 active site via docking experiments.

In experimental 3D structures of VIM-2 complexes with triazole-thione inhibitors (e. g. PDB codes 7PP0, 7OVF), the hydroxide anion is absent as the two zincs are coordinated by the S and N atoms of the triazole-thione moiety. This specific interaction leads to an increase of the distance between the two zincs (from 3.7 Å to 4.2 Å) (as seen in structures of complexes where the hydroxide anion is present, e.g. PDB codes 5ACW, 5LSC, 5NI0, 5NHZ, 6DD0, 6DD1, 6KW1, 6O5T, 6TGI, 6Y6J, 6YRP, 7A5Z, 7A60, 7OVE, 7OVF, 7OVH, 7PP0). Therefore, the docking was optimised to reflect this mode of binding allowing to grasp potential interactions of the compounds with the residues Arg228, Phe61 and Trp87, as a function of the nature of the substituents present at positions 4 and 5.

Therefore, the docking experiments were performed with a VIM-2 model generated from 7PP0[46] available in the Protein data bank using AutoDock VINA 1.2.0.[53] 7PP0 is the crystallographic structure of the complex formed between VIM-2 and the phenethyl analogue JMV7038 (K_i = 0.34 μM, Figure S1), which differs from **41** by possessing a phenyl ring *meta*-substituted with a flexible morpholinyl-ethoxy moiety and a 2-(*o*-benzoic)ethyl group at positions 5 and 4 of the triazole ring, respectively (Figure S1). The structure showed that the 1,2,4-triazole-3-thione core of JMV7038 simultaneously coordinated both active site zinc ions, displacing the catalytic hydroxide anion and increasing the distance Zn1-Zn2, as observed in other structures of 1,2,4-triazole-3-thione/VIM-2 complexes (PDB codes 6YRP, 5ACW, 6TGI, 7OVE, 7OVF, 7OVH). Among significant interactions, the carboxylate of the benzoic group is stabilized through H-bond with the Asn233 backbone nitrogen and by additional water mediated interactions. The benzoic phenyl ring also establishes a distorted π-π interaction with the His263 imidazole. The *m*-alkoxy phenyl substituent in position 5 adopts two orientations mutually rotated by ~ 180°. The phenyl moiety of both conformations is within van der Waals contact to the Trp87 indole. But the morpholinyl-ethyl group is located in the solvent exposed area and is too flexible to be resolved.

As already observed for the structure of VIM-2 in complex with the 1,2,4-triazole-3-thione Schiff base JMV4690 (PDB code 6YRP, [39] Figure S1), which also possesses a benzoic group at the same position as JMV7038, the close Arg228 does not make electrostatic interaction with the compound carboxylate groups. In fact, although expected, this interaction was prevented by the bulkiness of the benzoyl cycle. Interestingly, the same behaviour was observed for unrelated carboxylic-containing VIM-2 inhibitors (e. g. see PDB codes 4UA4, 5LCA, 5LM6, 5O7N). Indeed, their acidic function also interacted with the Asn233 backbone nitrogen and water molecules, while Arg228 kept the same position in all structures. Anyway, compound **56** also possesses a carboxylic group but not the two others **41** and **62**, the question arises as to whether the Arg228 side-chain should be let freely moving or fixed. Indeed, docking is strongly influenced by electrostatic interactions, which might inappropriately prevail over other ones. Therefore, docking was performed with free and fixed Arg228.

2.6.1. Method validation with JMV7038

We first docked the original ligand in VIM-2 to check that our

protocol allowed the crystallographic positioning. It was not possible when the arginine side-chain was let moving, as it favoured electrostatic interaction between the compound carboxylate and the arginine guanidinium. In contrast, blocking the arginine orientation seen in 7PP0.pdb allowed to very well reproduce the crystal pose, including the two opposite positionings of the 5-substituent (Fig. S2). Although the morpholinyl-ethyl moiety was not resolved in the crystal structure, the solvent-free docking proposed possible interactions between the morpholino oxygen atom with either the Tyr67 hydroxyl group (positioning 1) or the Asn150 NH_2 group (positioning 2).

2.6.2. Compound **41**

This compound is characterized by a *m*-biphenyl and a 2,4-dihydroxy-phenethyl substituents at positions 5 and 4, respectively. When the arginine side-chain was fixed, the correct positioning of the 1,2,4-triazole-3-thione core was prevented by conflicts occurring between the compound *p*-hydroxyl and biphenyl groups and Arg228 and Trp87, respectively. When the arginine was free, the 1,2,4-triazole-3-thione core could be more adequately placed. The 2,4-dihydroxyphenyl group could take two orientations, both of which interacting with Tyr67, while the biphenyl could establish π-stacking interaction with Phe61. However, some biphenyl orientations could clash with Trp87. When comparing all sixty-six VIM-2 structures available in the Protein Data Bank, the Trp87 position is highly conserved and rarely disturbed by a ligand. But it is the case in the presence of a triazolylthioacetamide inhibitor (PDB code 5LSC[54]). So, we used the 5LSC structure to dock compound **41** letting Arg228 free. In this case, the different orientation of Trp87 largely improved the positioning of the 1,2,4-triazole-3-thione core. In addition, the biphenyl group made interesting π-π stacking interactions with Phe61 and the *p*-hydroxyl group interacted with the Asp63 side-chain, which was further stabilized by the Tyr67 phenol group (Fig. 2A).

2.6.3. Compound **56**

This compound significantly differs from JMV7038 and compound **41** as the link between the triazole and the 4-substituent phenyl ring was one atom shorter, making this substituent less mobile. When the arginine was let flexible, the compound carboxylate group interacted with the Arg228 guanidinium and the Tyr67 hydroxyl group. However, this dominant interaction did not allow the correct positioning of the 1,2,4-triazole-3-thione core between the two zinc atoms. As observed with JMV7038 docking, fixing the arginine side-chain resolved the problem. In that case, no interaction between the compound carboxylate and Arg228 was established. The benzoic moiety displayed a different orientation compared to the JMV7038 one and established interactions with the same water molecules as well as Tyr67 (Fig. 2B).

2.6.4. Compound **62**

This compound is characterized by a four-atom long alkyl link and the absence of any functional groups on the two substituents. Whether arginine was free or not, no significant change was observed. The highly hydrophobic butylphenyl moiety was interacting within a hydrophobic zone delimited by Tyr67 and Phe61 aromatic rings (Fig. 2C).

Overall, it was possible to obtain for both compounds the conserved crystallographic positioning of the 1,2,4-triazole-3-thione that we assumed to be a prerequisite to MBL inhibition. Apart the zinc-binding moiety, the favoured poses of both substituents was significantly different than those observed for JMV7038 because of their structural distance (i.e. a bulky biphenyl group in **41** or a variable link size in **56** and **62**). In particular, while the benzoic group of JMV7038 (and also JMV4690) established hydrogen bonds in the Asn233 pocket, both 4-substituents of docked compounds were proposed to interact with or close to Tyr67, leading to important side-chain movement(s) in the hydrophobic patch including Phe61 and Tyr67 (Figure 2). This study afforded valuable information to further optimize these compounds.

The scores (i.e. binding affinity in kcal/mol) and ligand efficiencies

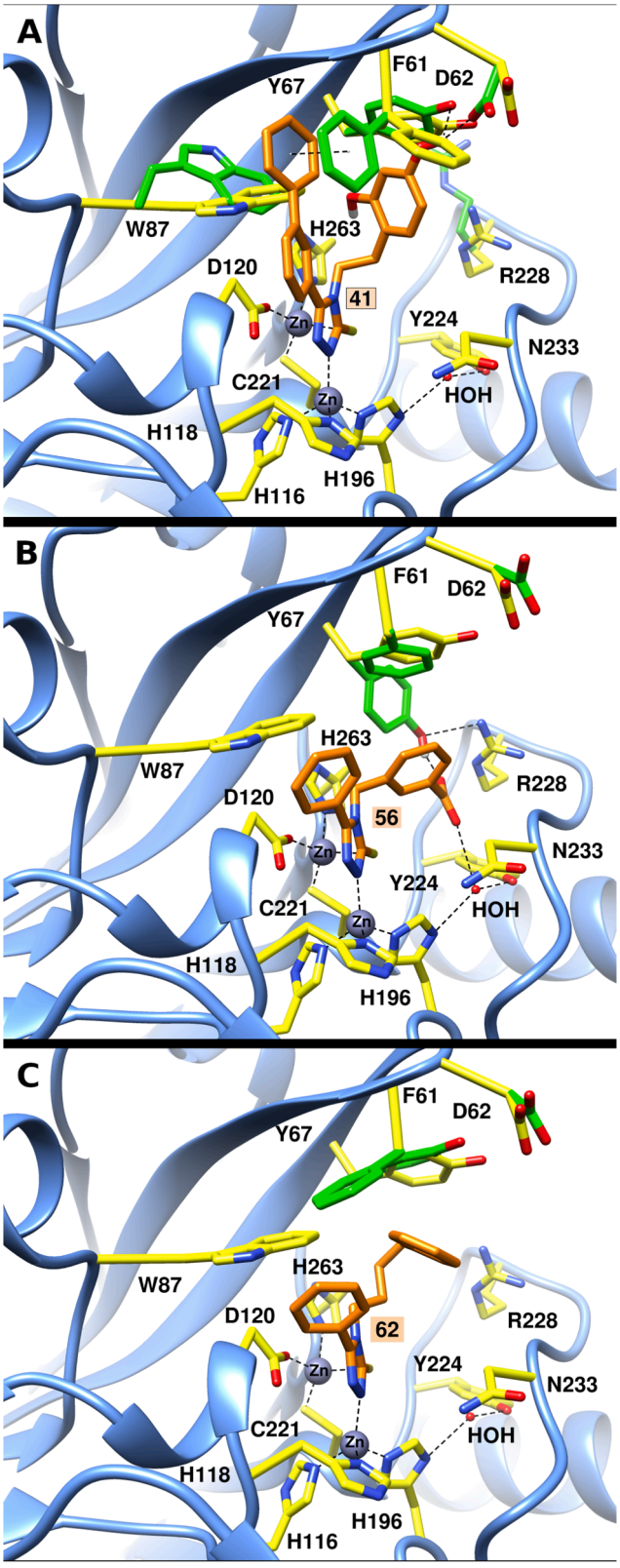

Figure 2. Binding mode of compounds **41** (A), **56** (B) and **62** (C) in VIM-2 (blue ribbon and yellow side chains) studied by molecular modeling. Compounds (orange) were docked using the structure 7PP0.pdb, excepted compound **41**, which used 5LSC.pdb. In the case of compound **62** (C), only the pose obtained with fixed Arg228 was shown. Protein side chains, which have moved from their position in 7PP0 (yellow) are in green. All three compounds interact with the two zinc ions as determined for JMV7038. The images were produced using UCSF Chimera. [55.]

(LE) were calculated for best poses and are presented in Table S1. The low ligand efficiency calculated for JMV7038 (0.20) compared to other compounds is probably due to the fact that a significant portion of its structure (i.e. the morpholinylethyl moiety) does not establish stable interaction with the VIM-2 active site.

3. Conclusion

When a direct comparison could be made with their corresponding Schiff base analogues (i.e. **15**, **21**, **26**–**28**, **38**, **41**, **50**), [39] the compounds presented in this study were globally better MBL inhibitors, with a few exceptions (i.e. **28**, **38**). In particular, compound **41** was much more potent against VIM-type enzymes and also inhibited NDM-1. When possible to compare with the 4-[2-(*o*-benzoic)ethyl] series, [46] which inhibition spectrum was restricted to VIM-type MBLs, the absence of the carboxylic group (i.e. unsubstituted phenethyl group at position 4 for compounds **15**, **26**, **29**, **34**) generally led to a decrease in inhibitory potency toward VIM-2. But importantly, in one case, a broader inhibition spectrum was observed as compound **29** also inhibited NDM-1 and IMP-1. In fact, several other compounds of the present series, all possessing at least one phenol group on the 4-substituent, showed broad-spectrum of inhibition (**20**, **41**–**43**).

Compared to previous series, while several aryl groups of substituents at position 4 were already known to be favourable for MBL inhibition (i.e. 2,4-dihydroxyphenyl and *p*-benzyloxyphenyl), other new moieties unsubstituted on their phenyl group were here shown useful. It is the case of phenylcyclopropyl (i.e. **18**, **30**) or isobenzofuranone (i.e. **25**, **33**, **37**, **48**). Furthermore, increasing the alkyl length to a propyl or a butyl yielded very potent VIM-type MBL inhibitors (**60** and **62**, respectively).

In contrast to the Schiff base analogues, which were devoid of synergistic activity when tested in clinical isolates in combination with a β-lactam antibiotic, [39] but as observed for the 4-[2-(*o*-benzoic)ethyl] series, [46] some compounds were able to potentiate the activity of meropenem against two VIM-producing clinical isolates of *K. pneumoniae*.

Therefore, because of its activity in bacteria and its potential to inhibit both VIM-type, NDM-1 and IMP-1 MBLs, this series deserves further development.

4. Experimental section

4.1. Chemistry

Hydrazides R^1-CO-$NHNH_2$ and amines R^2-NH_2 were prepared as described in Supplementary material part.

4.1.1. General procedure for the preparation of 4-alkyl-1,2,4-triazole-3-thiones diversely substituted at position 5

The procedure followed the synthetic pathway reported by Deprez-Poulain et al. [47].

4.1.1.1. Thiosemicarbazide intermediates. To a solution of the amine R^2-NH_2 (1 mmol, 1 equiv.) in anhydrous DMF (4 mL) (in the case of hydrochloride salt, 1.5 equiv. of Na_2CO_3 (159 mg) was added) was added DPT (244 mg, 1.05 mmol, 1.05 equiv.). The reaction mixture was stirred at 55 °C in a sealed tube for 1 h30. The hydrazide R^1-$CONHNH_2$ (1.1 mmol, 1.1 equiv.) was then added and the mixture was again heated at 55 °C for 1 h30, and allowed to cool to room temperature. The solution was diluted in EtOAc and the organic phase was extracted five times with water, dried over $MgSO_4$ and concentrated in vacuum. If necessary, the product was purified by gel column chromatography (EtOAc/Hexane).

4.1.1.2. Cyclization. The thiosemicarbazide intermediates were solubilized in a mixture of water and ethanol (2:3) and KOH (3 equiv., 3 mmol) was added. The reaction mixture was refluxed for 2 h. The mixture was then neutralized with saturated aqueous $KHSO_4$ and extracted twice with DCM. The organic phases were mixed, dried over $MgSO_4$, filtered and evaporated under vacuum. The residues were purified by gel column chromatography (EtOAc/Hexane), reverse phase HPLC or recrystallization.

The purity of all compounds was determined to be ≥ 95 % by ^{1}H NMR and LC-MS analysis. Their characteristics are presented in the Supplementary material part.

4.2. Biology

4.2.1. Metallo-β-Lactamase inhibition assays

4.2.1.1. VIM-type enzymes, NDM-1 and IMP-1. The inhibition potency of the compounds has been assessed as previously reported. [39,41] The rate of hydrolysis of a reporter substrate (150 μM imipenem or meropenem), by a purified MBL enzyme (VIM-1, VIM-2, VIM-4, NDM-1, and IMP-1; enzyme concentration in the assay ranged 1–70 nM) was measured at 30 °C in 50 mM HEPES buffer (pH 7.5) in the absence and presence of several concentrations of the inhibitor (0.5 μM –1 mM), by following the absorbance variation at λ = 300 nm.

The inhibition constants (K_i) were determined on the basis of a model of competitive inhibition by analysing the dependence of the ratio v_0/v_i (v_0, hydrolysis velocity in the absence of inhibitor; v_i, hydrolysis velocity in the presence of inhibitor) as a function of [I] as already described. [56] The slope of the plot of v_0/v_i *vs* [I], which corresponds to $K_m^S/(K_m^S + [S])$ K_i (where K_m^S is the K_m value of the reporter substrate and [S] its concentration in the reaction mixture) and allowed the calculation of the K_i value. Alternatively, a Dixon plot analysis was carried out by measuring the initial hydrolysis rates in the presence of variable concentrations of inhibitor and substrate. This allowed K_i values to be determined and supported the hypothesis that the various compounds behaved as competitive inhibitors of the various tested enzymes. The assays were performed in triplicate.

4.2.1.2. L1. L1 inhibition was measured as previously described. [39].

4.2.2. Microbiological assays

The minimum inhibitory concentrations (MICs) of meropenem (MEM) were determined using Mueller-Hinton broth and a bacterial inoculum of 5×10^4 CFU/well, as recommended by the CLSI, [57] in both the absence and presence of a fixed concentration (32 μg/ml) of an inhibitor, as previously described. [41,46] VIM-1- and VIM-4-producing *K. pneumoniae* (strains 7023 and VA-416/02, respectively) and NDM-1-producing *Escherichia coli* (SI-004 M) clinical isolates present in our collection were used. Chequerboard analysis, used to confirm the nature of the interaction between meropenem and selected active inhibitors (synergistic *vs* additive activity), was carried out and interpreted as previously described. [41] All experiments were performed in triplicate.

4.2.3. Angiotensin-converting enzyme (ACE) inhibition assays

The potential inhibitory activity of compounds on the Zn-dependent ACE was determined essentially as described in Sentandreu and Toldrá. [58] ACE enzyme from rabbit lung was purchased from Sigma (St Louis, Miss., USA; cat. no. A6778). The fluorogenic tripeptide substrate *o*-aminobenzoylglycyl-*p*-nitro-L-phenylalanyl-L-proline (Abz-Gly-Phe(NO_2)-Pro) [59] was purchased from FluoProbes (Interchim, Montluçon, France). The enzyme was resuspended at 0.3 U/mL (≈150 μg/mL) in 150 mM Tris (pH, 8.3), 1 μM $ZnCl_2$, 50 % glycerol buffer and kept at −20 °C until use. Fluorescence of the reaction product Abz-Gly-OH (i. e. generated after cleavage of the peptide with ACE) was measured in the reaction buffer (150 mM Tris, 750 mM NaCl, pH 8.3) using a monochromators-equipped Envision microplate reader (Perkin-Elmer, Waltham, Mass., USA) and excitation and emission wavelengths of 316

and 413 nm, respectively. Purified Abz-Gly-OH was used to establish the linearity between measured fluorescence and product concentration (range, 0–50 μM) in the reaction buffer. The rate of hydrolysis of the fluorogenic substrate was measured in both the absence (v_0) and presence (v_i) of 100 μM compound by monitoring the increase of blank-corrected fluorescence for up to 90 min, in the reaction buffer (final reaction volume, 300 μL) and 1.5 mUnits of ACE per well. The percentage of inhibition was computed as 100 - [(v_i/v_o) × 100]. Controls included substrate alone and reactions in the presence of 100 nM captopril, a well-known potent inhibitor of ACE.

4.2.4. Cell toxicity assay

The potential cytotoxic activity of compound **41** was evaluated on HeLa cell cultures using the commercially available membrane integrity assay (CytoTox 96® non-radioactive cytotoxicity assay, Promega, Madison, WI, U.S.A.) as previously described. [39] The cytotoxicity of compounds was also assessed using the RealTime-Glo™ MT Cell Viability Assay (Promega). [39] The assays were performed in triplicate.

4.3. Molecular modelling

The geometric optimization of the compound structures was done using Gaussian 16 at DFT level of theory with B3LYP hybrid functional and 6–31 g basis set. The resulting structures were registered as mol2 files. AM1 charges were calculated using Chimera software and Antechamber. Then, in AutoDockTools (ADT), [60] the final files (pdbqt) were generated where AM1 charges were kept and all possible rotations were free.

The docking studies were performed with AutoDock Vina 1.2.0. [53] This new version allows docking on zinc metallo-enzymes. The method consists in placing fictional points (TZ) to complete the Zn coordination spheres. They will serve to anchor the 1,2,4-triazole-3-thione core of the ligands. Files for the docking were prepared from: (i) the structure of complex VIM-2/JMV7038 (PDB code 7PP0), [46] which was treated as follows: water molecules (with the exception of structural waters 5 and 177, small molecules (acetate, DMSO and ethylene glycol) and the third zinc ion were removed; The protein was protonated with Dockprep module of Chimera and the program was let to itself protonate His residues, while checking the absence of conflict in the H-bond network; AM1 charges were calculated using Chimera [55] and Antechamber and the file was registered as mol2 format. The center and dimensions of the docking grid box were obtained using ADT software and the size of the search zone was 30 Å x 30 Å x 30 Å. The structure 5LSC.pdb, [54] which was also used for compound **41** was similarly treated; (ii) compounds and protein pdbqt files prepared with ADT. For the protein, the side-chain of Arg228 was let free or fixed.

Molecular graphics and analyses were performed with UCSF Chimera, developed by the Resource of Biocomputing, Visualization and Informatics at the University of California, San Francisco, with support from NIH *P*41-GM103311.

Declaration of Competing Interest

The authors declare that they have no known competing financial interests or personal relationships that could have appeared to influence the work reported in this paper.

Data availability

Data will be made available on request.

Acknowledgments

Part of this work was supported by *Agence Nationale de la Recherche* (ANR-14-CE16-0028-01, including fellowship to L.S.). We thank Mr Pierre Sanchez for mass spectrometry analyses.

Appendix A. Supplementary material

Supplementary data to this article can be found online at https://doi.org/10.1016/j.bmc.2022.116964.

References

[1] Nordmann P, Naas T, Poirel L. Global spread of carbapenemase-producing Enterobacteriaceae. *Emerg Infect Dis*. 2011;17:1791–1798. https://doi.org/10.3201/eid1710.110655.
[2] Walsh TR, Toleman MA. The emergence of pan-resistant Gram-negative pathogens merits a rapid global political response. *J Antimicrob Chemother*. 2012;67:1–3. https://doi.org/10.1093/jac/dkr378.
[3] Reygaert WC. An overview of the antimicrobial resistance mechanisms of bacteria. *AIMS Microbiol*. 2018;4:482–501. https://doi.org/10.3934/microbiol.2018.3.482.
[4] World Health Organization, Global priority list of antibiotic-resistant bacteria to guide research, discovery and development of new antibiotics, 27 february 2017.
[5] Tooke CL, Hinchliffe P, Bragginton EC, et al. β-Lactamases and β-lactamase inhibitors in the 21st century. *J Mol Biol*. 2019;431:3472–3500. https://doi.org/10.1016/j.jmb.2019.04.002.
[6] Bush K. Past and present perspectives on β-lactamases. *Antimicrob Agents Chemother*. 2018;62:e01076–e10118. https://doi.org/10.1128/AAC.01076-18.
[7] Bahr G, Gonzalez LJ, Vila AJ. Metallo-β-lactamase inhibitors in the age of multidrug resistance: from structure and mechanism to evolution, dissemination, and inhibitor design. *Chem Rev*. 2021;121:7957–8094. https://doi.org/10.1021/acs.chemrev.1c00138.
[8] Palzkill T. Metallo-β-lactamase structure and function. *Ann N Y Acad Sci*. 2013;1277:91–104. https://doi.org/10.1111/j.1749-6632.2012.06796.x.
[9] Gajamer VR, Bhattacharjee A, Paul D, et al. *Escherichia coli* encoding bla_{NDM-5} associated with community-acquired urinary tract infections with unusual MIC creep-like phenomenon against imipenem. *J Glob Antimicrob Resist*. 2018;14:228–232. https://doi.org/10.1016/j.jgar.2018.05.004.
[10] Docquier J-D, Mangani S. An update on β-lactamase inhibitor discovery and development. *Drug Resist Updat*. 2018;36:13–29. https://doi.org/10.1016/j.drup.2017.11.002.
[11] Gonzalez-Bello C, Rodriguez D, Pernas M, Rodriguez A, Colchon E. β-Lactamase inhibitors to restore the efficacy of antibiotics against superbugs. *J Med Chem*. 2020;63:1859–1881. https://doi.org/10.1021/acs.jmedchem.9b01279.
[12] McGeary RP, Tan DT, Schenk G. Progress toward inhibitors of metallo-β-lactamases. *Future Med Chem*. 2017;9:673–691. https://doi.org/10.4155/fmc-2017-0007.
[13] Palacios AR, Rossi M-A, Mahler GS, Vila AJ. Metallo-β-lactamase inhibitors inspired on snapshots from the catalytic mechanism. *Biomolecules*. 2020;10:854. https://doi.org/10.3390/biom10060854.
[14] Yan Y-H, Li G, Li G-B. Principles and current strategies targeting metallo-β-lactamases mediated antibacterial resistance. *Med Res Rev*. 2020;40:1558–1592. https://doi.org/10.1002/med.21665.
[15] Liénard BM, Garau G, Horsfall L, et al. Structural basis for the broad-spectrum inhibition of metallo-β-lactamases by thiols. *Org Biomol Chem*. 2008;6:2282–2294. https://doi.org/10.1039/b802311e.
[16] Lassaux P, Hamel M, Gulea M, et al. Mercaptophosphonate compounds as broad-spectrum inhibitors of the metallo-β-lactamases. *J Med Chem*. 2010;53:4862–4876. https://doi.org/10.1021/jm100213c.
[17] Gonzalez MM, Kosmopoulou M, Mojica MF, et al. Bisthiazolidines: a substrate-mimicking scaffold as an inhibitor of the NDM-1 carbapenemase. *ACS Inf Dis*. 2015;1:544–554. https://doi.org/10.1021/acsinfecdis.5b00046.
[18] Kaya C, Konstantinović J, Kany AM, et al. *N*-Aryl mercaptopropionamides as broad-spectrum inhibitors of metallo-β-lactamases. *J Med Chem*. 2022;65:3913–3922. https://doi.org/10.1021/acs.jmedchem.1c01755.
[19] Toney JH, Hammond GG, Fitzgerald PM, et al. Succinic acids as potent inhibitors of plasmid-borne IMP-1 metallo-β-lactamase. *J Biol Chem*. 2001;276:31913–31918. https://doi.org/10.1074/jbc.M104742200.
[20] Chen AY, Thomas PW, Stewart AC, et al. Dipicolinic acid derivatives as inhibitors of New Delhi Metallo-β-lactamase-1. *J Med Chem*. 2017;60:7267–7283. https://doi.org/10.1021/acs.jmedchem.7b00407.
[21] King AM, Reid-Yu SA, Wang W, et al. Aspergillomarasmine A overcomes metallo-β-lactamase antibiotic resistance. *Nature*. 2014;510:503–506. https://doi.org/10.1038/nature13445.
[22] Bergstrom A, Katko A, Adkins Z, et al. Probing the interaction of aspergillomarasmine A with metallo-β-lactamase NDM-1, VIM-2, and IMP-7. *ACS Infect Dis*. 2018;4:135–145. https://doi.org/10.1021/acsinfecdis.7b00106.
[23] Samuelsen O, Astrand OAH, Fröhlich C, et al. ZN148 is a modular synthetic metallo-β-lactamase inhibitor that reverses carbapenem-resistance in Gram-negative pathogens *in vivo*. *Antimicrob Agents Chemother*. 2020;64:e02415–e2509. https://doi.org/10.1128/AAC.02415-19.
[24] Chen AY, Adamek RN, Dick BL, Credille CV, Morrison CN, Cohen SM. Targeting metalloenzymes for therapeutic intervention. *Chem Rev*. 2019;119:1323–1455. https://doi.org/10.1021/acs.chemrev.8b00201.
[25] Reddy N, Shungube M, Arvidsson PI, et al. A 2018–2019 patent review of metallo-β-lactamase inhibitors. *Expert Opin Ther Pat*. 2020;30:541–555. https://doi.org/10.1080/13543776.2020.1767070.
[26] Davies DT, Leiris S, Sprynski N, et al. ANT2681: SAR studies leading to the identification of a metallo-lactamase inhibitor with potential for clinical use in combination with meropenem for the treatment of infections caused by NDM-

producing Enterobacteriaceae. *ACS Infect Dis*. 2020;6:2419–2430. https://doi.org/10.1021/acsinfecdis.0c00207.
[27] Burns CJ, Daigle D, Liu B, McGarry D, Pevear DC, Trout RE. β-Lactamase inhibitors. *WO Patent WO*. 2014:089365A1.
[28] Krajnc A, Brem J, Hinchliffe P, et al. Bicyclic boronate VNRX-5133 inhibits metallo- and serine β-lactamases. *J Med Chem*. 2019;62:8544–8556. https://doi.org/10.1021/acs.jmedchem.9b00911.
[29] Liu B, Trout REL, Chu GH, et al. Discovery of Taniborbactam (VNRX-5133): a broad spectrum serine- and metallo-β-lactamase inhibitor for carbapenem-resistant bacterial infections. *J Med Chem*. 2020;63:2789–2801. https://doi.org/10.1021/acs.jmedchem.9b01518.
[30] Hamrick JC, Docquier JD, Uehara T, et al. VNRX-5133 (Taniborbactam), a broad-spectrum inhibitor of serine- and metallo-β-lactamase, restores activity of cefepime in Enterobacterales and *Pseudomonas aeruginosa*. *Antimicrob Agents Chemother*. 2020;64:e01963–e2019. https://doi.org/10.1128/AAC.01963-19.
[31] Hecker SJ, Reddy KR, Lomovskaya O, et al. Discovery of cyclic boronic acid QPX7728, an ultra-broad-spectrum inhibitor of serine and metallo-β-lactamases. *J Med Chem*. 2020;63:7491–7507. https://doi.org/10.1021/acs.jmedchem.9b01976.
[32] Olsen L, Jost S, Adolph HW, Pettersson I, Hemmingsen L, Jørgensen FS. New leads of metallo-β-lactamase inhibitors from structure-based pharmacophore design. *Bioorg Med Chem*. 2006;14:2627–2635. https://doi.org/10.1016/j.bmc.2005.11.046.
[33] Toney JH, Fitzgerald PM, Grover-Sharma N, et al. Antibiotic sensitization using biphenyl tetrazoles as potent inhibitors of *Bacteroides fragilis* metallo-beta-lactamase. *Chem Biol*. 1998;5:185–196. https://doi.org/10.1016/s1074-5521(98)90632-9.
[34] Hussein WM, Fatahala SS, Mohamed ZM, et al. Synthesis and kinetic testing of tetrahydropyrimidine-2-thione and pyrrole derivatives as inhibitors of the metallo-β-lactamase from *Klebsiella pneumonia* and *Pseudomonas aeruginosa*. *Chem Biol Drug Des*. 2012;80:500–515. https://doi.org/10.1111/j.1747-0285.2012.01440.x.
[35] Zhai L, Zhang YL, Kang JS, et al. Triazolylthioacetamide: a valid scaffold for the development of New Delhi Metallo-β-Lactamase-1 (NDM-1) inhibitors. *ACS Med Chem Lett*. 2016;7:413–417. https://doi.org/10.1021/acsmedchemlett.5b00495.
[36] Muhammad Z, Skagseth S, Boomgaren M, et al. Structural studies of triazole inhibitors with promising inhibitor effects against antibiotic resistance metallo-β-lactamases. *Bioorg Med Chem*. 2020;28, 115598. https://doi.org/10.1016/j.bmc.2020.115598.
[37] Nauton L, Kahn R, Garau G, Hernandez J-F, Dideberg O. Structural insights into the design of inhibitiors of the L1 metallo-β-lactamase from *Stenotrophomonas maltophilia*. *J Mol Biol*. 2008;375:257–269. https://doi.org/10.1016/j.jmb.2007.10.036.
[38] Christopeit T, Carlsen TJ, Helland R, Leiros HK. Discovery of novel inhibitor scaffolds against the metallo-β-lactamase VIM-2 by surface plasmon resonance (SPR) based fragment screening. *J Med Chem*. 2015;58:8671–8682. https://doi.org/10.1021/acs.jmedchem.5b01289.
[39] Gavara L, Sevaille L, De Luca F, et al. 4-Amino-1,2,4-triazole-3-thione-derived Schiff bases as metallo-β-lactamase inhibitors. *Eur J Med Chem*. 2020;208, 112720. https://doi.org/10.1016/j.ejmech.2020.112720.
[40] Spyrakis F, Santucci M, Maso L, et al. Virtual screening identifies broad-spectrum β-lactamase inhibitors with activity on clinically relevant serine- and metallo-carbapenemases. *Sci Rep*. 2020;10:12763. https://doi.org/10.1038/s41598-020-69431-y.
[41] Legru A, Verdirosa F, Hernandez J-F, et al. 1,2,4-Triazole-3-thione compounds with a 4-ethyl alkyl/aryl sulfide substituent are broad-spectrum metallo-β-lactamase inhibitors with re-sensitization activity. *Eur J Med Chem*. 2021;226, 113873. https://doi.org/10.1016/j.ejmech.2021.113873.
[42] Vella P, Hussein WM, Leung EW, et al. The identification of new metallo-β-lactamase inhibitor leads from fragment-based screening. *Bioorg Med Chem Lett*. 2011;21:3282–3285. https://doi.org/10.1016/j.bmcl.2011.04.027.
[43] Spyrakis F, Celenza G, Marcoccia F, et al. Structure-based virtual screening for the discovery of novel inhibitors of New Delhi Metallo-β-lactamase-1. *ACS Med Chem Lett*. 2018;9:45–50. https://doi.org/10.1021/acsmedchemlett.7b00428.
[44] Gavara L, Verdirosa F, Legru A, et al. 4-(*N*-Alkyl- and -acyl-amino)-1,2,4-triazole-3-thione analogs as metallo-β-lactamase inhibitors: impact of 4-linker on potency and spectrum of inhibition. *Biomolecules*. 2020;10:1094. https://doi.org/10.3390/biom10081094.
[45] Gavara L, Legru A, Verdirosa F, et al. 4-Alkyl-1,2,4-triazole-3-thione analogues as metallo-β-lactamase inhibitors. *Bioorg Chem*. 2021;113, 105024. https://doi.org/10.1016/j.bioorg.2021.105024.
[46] Verdirosa F, Gavara L, Sevaille L, et al. 1,2,4-Triazole-3-thione analogues with a 2-ethylbenzoic acid at position 4 as VIM-type metallo-β-lactamase inhibitors. *ChemMedChem*. 2022;17, e202100699. https://doi.org/10.1002/cmdc.202100699.
[47] Deprez-Poulain RF, Charton J, Leroux V, Deprez BP. Convenient synthesis of 4*H*–1,2,4-triazole-3-thiols using di-2-pyridylthionocarbamate. *Tetrahedron Lett*. 2007;48:8157–8162. https://doi.org/10.1016/j.tetlet.2007.09.094.
[48] Sevaille L, Gavara L, Bebrone C, et al. 1,2,4-Triazole-3-thione compounds as inhibitors of dizinc metallo-β-lactamase. *ChemMedChem*. 2017;12:972–985. https://doi.org/10.1002/cmdc.201700186.
[49] Akiyama T, Hirofuji H, Ozaki S. $AlCl_3$-*N*, N-dimethylaniline: a new benzyl and allyl ether cleavage reagent. *Tetrahedron Lett*. 1991;32:1321–1324. https://doi.org/10.1016/S0040-4039(00)79656-0.
[50] Negash KH, Norris JKS, Hodgkinson JT. Siderophore-antibiotic conjugate design: new drugs for bad bugs? *Molecules*. 2019;24:3314. https://doi.org/10.3390/molecules24183314.
[51] European Committee for Antimicrobial Susceptibility Testing (EUCAST) of the European Society of Clinical Microbiology and Infectious Diseases (ESCMID). EUCAST Definitive Document E.Def 1.2. Terminology relating to methods for the determination of susceptibility of bacteria to antimicrobial agents. Clin Microb Infect. 2000; 6: 503-508. DOI: 10.1046/j.1469-0691.2000.00149.x.
[52] Sentandreu MA, Toldrá F. A rapid, simple and sensitive fluorescence method for the assay of angiotensin-I converting enzyme. *Food Chem*. 2006;97:546–554. https://doi.org/10.1016/j.foodchem.2005.06.006.
[53] Eberhardt J, Santos-Martins D, Tillack AF, Forli S. AutoDock Vina 1.2.0: New docking methods, expanded force field, and python bindings. *J Chem Inf Model*. 2021;61:3891–3898. https://doi.org/10.1021/acs.jcim.1c00203.
[54] Christopeit T, Yang KW, Yang SK, Leiros HKS. The structure of the metallo-β-lactamase VIM-2 in complex with a triazolylthioacetamide inhibitor. *Acta Crystallogr. F*. 2016;72:813–819. https://doi.org/10.1107/S2053230X16016113.
[55] Pettersen EF, Goddard TD, Huang CC, et al. UCSF Chimera, a visualization system for exploratory research and analysis. *J Comput Chem*. 2004;25:1605–1612. https://doi.org/10.1002/jcc.20084.
[56] Docquier J-D, Lamotte-Brasseur J, Galleni M, Amicosante G, Frère J-M, Rossolini GM. On functional and structural heterogeneity of VIM-type metallo-β-lactamases. *J Antimicrob Chemother*. 2003;51:257–266. https://doi.org/10.1093/jac/dkg067.
[57] Clinical Laboratory Standard Institute, Methods for dilution antimicrobial susceptibility tests for bacteria that grow aerobically, Document M07-A10, 2015, Twelfth Edition, Wayne, PA, USA.
[58] Sentandreu MA, Toldrá F. A fluorescence-based protocol for quantifying angiotensin-converting enzyme activity. *Nat Protoc*. 2006;1:2423–2427. https://doi.org/10.1038/nprot.2006.349.
[59] Carmel A, Yaron A. An intramolecularly quenched fluorescent tripeptide as a fluorogenic substrate of angiotensin-I-converting enzyme and of bacterial dipeptidyl carboxypeptidase. *Eur J Biochem*. 1978;87:265–273. https://doi.org/10.1111/j.1432-1033.1978.tb12375.x.
[60] Sanner MF. Python: a programming language for software integration and development. *J Mol Graph Model*. 1999;17:57–61. PMID: 10660911.